JOURNAL OF MATERIALS SCIENCE 17 (1982) 417–428

Tensile fracture of centre-notched angle ply $(0/\pm 45/0)_S$ and $(0/90)_{2S}$ graphite-epoxy composites

S. OCHIAI*, P. W. M. PETERS
DFVLR, Institut für Werkstoff-Forschung, Postfach 90 60 58, D-5000 Köln 90, West Germany

The fracture behaviour of centre-notched $(0/\pm 45/0)_S$ and $(0/90)_{2S}$ laminates with increasing notch length has been studied. Two test series have been investigated: specimens of constant width ($W = 20$ mm) and small notch length ($2a \leqslant 12$ mm), and specimens with various notch lengths ($5 \leqslant 2a \leqslant 35$ mm) and a constant relative notch length ($2a/W = 0.5$). An X-ray technique showed that the damage at the notch tip, which is formed at increasing load, consists mainly of subcracks parallel to the fibres of the constituent layers. The damage zone causes the crack opening displacement (COD) to deviate from the original linearity. The K_R curve concept has been applied assuming that the COD deviation from linearity is completely the result of original crack extension. This approach fails to describe the notch length effect, because a tangent point between the K_R and K curves was not found and because of a strong dependency of the maximum fracture resistance $K_{R\,max}$ on notch length. The fracture behaviour of 20 mm wide specimens could be explained with the point and average stress criteria, based on characteristic lengths which are independent of notch length. At various notch lengths at a constant $2a/W = 0.5$, however, the characteristic lengths increased with increasing notch length.

1. Introduction

A great deal of effort has been made to characterize the fracture behaviour of composites [1–8]. Two different approaches have been offered to explain the well-known phenomenon that larger holes (notches) cause greater fracture stress reductions than smaller holes (notches), which cannot be explained by a critical stress concentration factor. These approaches are the model of Waddoups *et al.* [1] (the WEK model) and the point and average stress criteria [4, 5]. The WEK model assumes the existence of an intense energy (inherent flaw) region with a size of a^* which is modelled as a through crack of constant length, extending perpendicular to the load direction. Waddoups *et al.* [1] obtained reasonable correlation between experimental data and the WEK model.

In the point and average stress criteria, Whitney and Nuismer [4, 5] proposed a failure model based on the theoretical stress distribution near the notch tip, assuming that failure occurs when the stress over some distance d_0 in front of the notch tip is equal to or greater than the strength of unnotched material (point stress criterion) or when the average stress over some distance a_0 equals the unnotched strength (average stress criterion). Both characteristic dimensions d_0 and a_0 were assumed to be material properties independent of laminate construction and stress distribution. The average stress criterion was shown to be identical to the WEK model, since the inherent flaw size a^* in the WEK model is equal to $a_0/2$ [9]. The values of d_0, a^* and a_0 have been shown by most workers to be independent of hole or notch

*Present address: Department of Metallurgy, Faculty of Engineering, Kyoto University, Sakyo-ku, Kyoto 606, Japan.

0022–2461/82/020417–12$3.20/0

size [1–5], although Prabhakaran [10] has reported that the characteristic lengths depend on the hole size. One of the aims of the present work on graphite–epoxy is to see whether and to what extent the characteristic lengths depend on the notch length and specimen size.

Composites with brittle resins and brittle fibres do not deform plastically but a damage zone arises at the notch tip in the form of cracking along the fibre directions within plies and delamination between plies. This suggests that an energy absorption mechanism exists in composites as well as in metals in which plastic flow takes place at the notch tip.

Gagger and Broutman [6] and Morris and Hahn [7] demonstrated the possibility of using the resistance method (K_R curve method) as a means of characterizing the fracture resistance of composites by showing that the K_R curve is independent of the initial crack length. Morris and Hahn [7] and Kim [11] applied the K_R curve concept and found that the quasi-self-similar crack extension at fracture Δa_f is almost equal to the characteristic length d_0 of the point stress criterion.

The extension of the damage zone has been shown to influence the fracture toughness of composites. A further aim of this work is to investigate experimentally the extension of the damage zone and its relation to the fracture toughness of graphite–epoxy composites and to examine the applicability of the WEK model, the point and average stress criteria and the K_R curve method.

2. Materials and experimental procedure

The composite plates were prepared by DFVLR Braunschweig from T300/Code 69 or T300/914C prepreg. The nominal thickness and fibre volume fraction of the prepreg were 0.125 mm and 60%, respectively. The investigated laminates and specimen types are given in Table I. "0" refers to the longitudinal direction and "± 45" and "90" refer to the inclinations from the "0" direction. "s" means a symmetric repetition of the sequency given in the parentheses. The ultimate tensile strength (out of three 10 mm wide specimens) has only been measured on the laminates with a 914C matrix. They show a minor difference in strength between the two laminates. The influence of the crack length on fracture behaviour was investigated on centre-notched (CN) specimens. Notch lengths of $0 < 2a \leqslant 12$ mm were introduced into 20 mm wide specimens, whereas the effect of various notch lengths ($5 \leqslant 2a \leqslant 35$ mm) was investigated on specimens with a constant relative crack length, $2a/W = 0.5$

Specimens were cut out of the plates supplied (300 mm × 300 mm) with a diamond wheel. Cracks with various lengths were introduced first by drilling a small pilot hole in the specimen, followed by lengthening with a 0.35 mm steel saw or a 0.25 mm diamond wire. No attempt was made to sharpen the crack tips further, since this method has been shown to give a sufficiently sharp notch for valid fracture toughness testing for this type of material [12].

Aluminium sheet was attached at end tabs with a length of 40 mm. The ratio of the free length between the grips to the specimen width, L/W, was 3 to 5 for all notched specimens. The cross-head speed was 0.4 mm min^{-1}. During each test, the applied load and crack opening displacement (COD) were monitored and recorded continuously. The COD was measured on the centre lines of the specimen with clip gauges attached to the front and back surfaces. The gauges of the clip gauge measured 10.5 mm. The mean values of COD measured on both surfaces are used as COD values in the analysis. Compliance calibration based on COD, as a function of initial crack length, was obtained from the initial straight portion of a load–COD curve. Crack growth resistance K_R was determined by compliance matching, as described in [6, 7, 11]. Some of the specimens were loaded to a given K (stress intensity factor) value and after unloading were examined with X-rays [13] to monitor the growth of the damage zone. A tetra-

TABLE I The laminates investigated and specimen types

Laminate	Matrix	Ultimate tensile stress σ_U (MPa)	Centre-notched $0 < 2a \leqslant 12$ mm $W = 20$ mm	Centre-notched $5 \leqslant 2a \leqslant 35$ mm $2a/W = 0.5$
$(0/\pm 45/0)_s$	Code 69		X	
	914 C	932		X
$(0/90)_{2s}$	Code 69		X	
	914 C	920		X

bromoethane opaque was applied at the sources of the damage zones to enhance the flaw image.

3. Results and discussion

3.1. Stress–COD curves

Fig. 1 depicts typical stress–COD curves for $(0/\pm 45/0)_s$ and $(0/90)_{2s}$ specimens with various notch lengths. In the $(0/\pm 45/0)_s$ specimens, the COD increased suddenly at higher stress levels. On the other hand, in $(0/90)_{2s}$ specimens, the shape of the curves was relatively smooth. This implies that in the $(0/\pm 45/0)_s$ composite a sudden extension of the damage zone occured, whereas in the $(0/90)_{2s}$ composite the damage zone extended gradually.

Another difference between $(0/\pm 45/0)_s$ and $(0/90)_{2s}$ composites was that the COD values at fracture were higher in the $(0/90)_{2s}$ laminate than in the $(0/\pm 45/0)_s$ laminate at a given crack length. This suggests that the extension of the crack or the crack tip damage zone in $(0/90)_{2s}$ composite was larger than those in $(0/\pm 45/0)_s$ composite. It is obvious that the larger the notch, the larger the COD at fracture for both the laminates.

3.2. Tensile strength and stress intensity factor at fracture

From the failure load of the unnotched and notched specimens, the failure stresses σ_U and σ_N, respectively, were obtained. The finite-width correction factor for the angle ply laminate composite is different from the isotropic value. However, the difference is less than a few per cent [14, 15]. Therefore, an infinite-width plate failure stress σ_N^∞ was obtained for all laminates by multiplying σ_N by the isotropic finite-width correction factor of Fedderson [16],

$$Y = [\sec(\pi a/W)]^{1/2}. \quad (1)$$

The notched, infinite-width failure stress for each notched specimen was normalized by dividing by the average unnotched tensile strength, that is, the ratio σ_N^∞/σ_U was calculated. The stress intensity factor K_{max} at failure was calculated by using

$$K_{max} = Y\sigma_N(\pi a)^{1/2}. \quad (2)$$

First the results of CN (centre-notched) specimens ($W = 20$ mm) with varying crack length $2a$ will be discussed. Fig. 2 presents the measured values of σ_N^∞/σ_U and K_{max} plotted against $2a/W$ of the $(0/\pm 45/0)_s$ and $(0/90)_{2s}$ composites. As the tensile strength of the T300/Code 69 laminates is unknown, the tensile strength of the corresponding laminates made from T300/914C material has been used (Table I). The difference in tensile strength can be expected to be low. According to the point and average stress criteria [4, 5], σ_N^∞/σ_U of centre-notched specimens is given by

$$\sigma_N^\infty/\sigma_U = \{1 - [a/(a + d_0)]^2\}^{1/2} \quad (3)$$

for the point stress criterion and

$$\sigma_N^\infty/\sigma_U = \left(\frac{1 - a/(a + a_0)}{1 + a/(a + a_0)}\right)^{1/2} \quad (4)$$

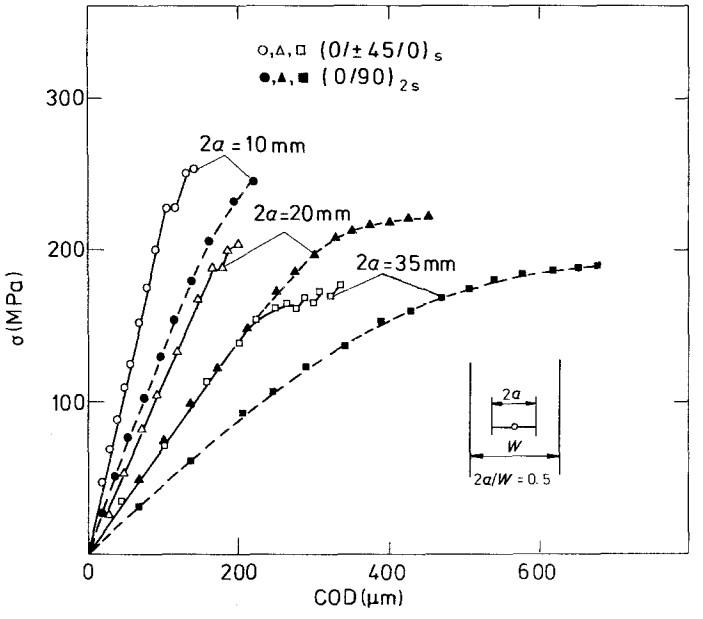

Figure 1 Gross stress–COD curves of centre-notched $(0/\pm 45/0)_s$ and $(0/90)_{2s}$ specimens with different notch lengths $2a$ at a constant $2a/W = 0.5$.

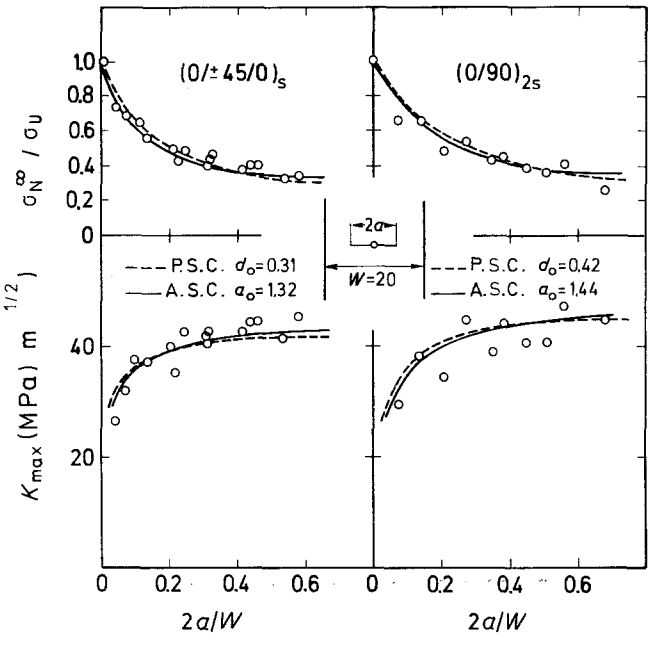

Figure 2 The dependency of the non-dimensionalized fracture stress σ_N^∞/σ_U and the fracture toughness K_{max} with the relative notch length $2a/W$ at a constant W = 20 mm.

for the average stress criterion. K_{max} is given by

$$K_{max} = \sigma_U(\pi a\{1 - [a/(a + d_0)]^2\})^{1/2} \quad (5)$$

for the point stress criterion and

$$K_{max} = \sigma_U\left(\frac{\pi a[1 - a/(a + a_0)]}{1 + a/(a + a_0)}\right)^{1/2} \quad (6)$$

for the average stress criterion. The values of the characteristic lengths d_0 and a_0 of each specimen were calculated using Equations 3 and 4. The average characteristic lengths were $d_0 = 0.31$ mm and $a_0 = 1.32$ mm for the $(0/\pm 45/0)_s$ and $d_0 = 0.42$ mm and $a_0 = 1.74$ mm for the $(0/90)_{2s}$ laminate. After substitution the characteristic lengths in Equation 3–6, the dependency of the normalized fracture stress σ_N^∞/σ_U and the toughness K_{max} on the relative notch length $2a/W$ is presented in Fig. 2 by the broken (point stress criterion) and full curves (average stress criterion). These curves seem to fit well with the experimental results, which indicate that the point and average stress criteria are applicable. Unfortunately, the scatter of the characteristic length value is very large, as shown in Fig. 3, much larger than the scatter in the test results of Fig. 2.

Can the point and average stress criteria describe the influence of varying notch length? To answer this question, specimens with notch length up to $2a = 35$ mm at a constant relative notch length $2a/W = 0.5$ were tested. Fig. 4 shows that for both $(0/\pm 45/0)_s$ and $(0/90)_{2s}$ laminates the increase in toughness K_{max} (Equation 2) with rising notch length is rather strong. This has also been found by Mandell *et al.* [17] for some graphite–epoxy laminates. The characteristic lengths d_0 and a_0 of each specimen were calculated by using Equations 5 and 6. The result is given in Fig. 5. It is obvious that d_0 as well as a_0 increases with increasing notch length $2a$. The rather steep increase of the toughness, and consequently the characteristic length, at smaller

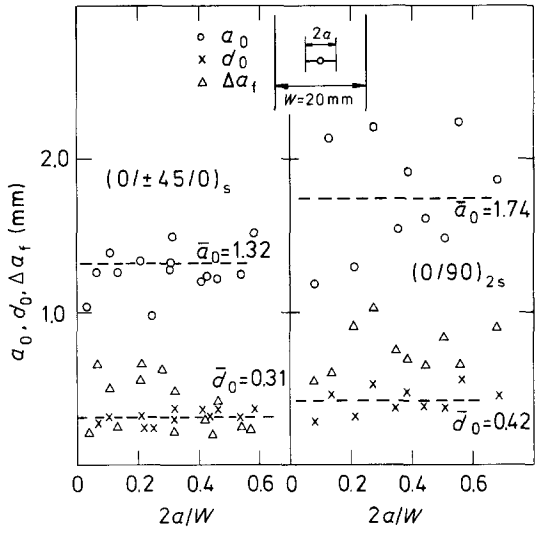

Figure 3 The characteristic lengths a_0, d_0 and the (quasi) crack extension at fracture Δa_f of centre-notched $(0/\pm 45/0)_s$ and $(0/90)_{2s}$ specimens (W = 20 mm) plotted against the ralative notch length $2a/W$.

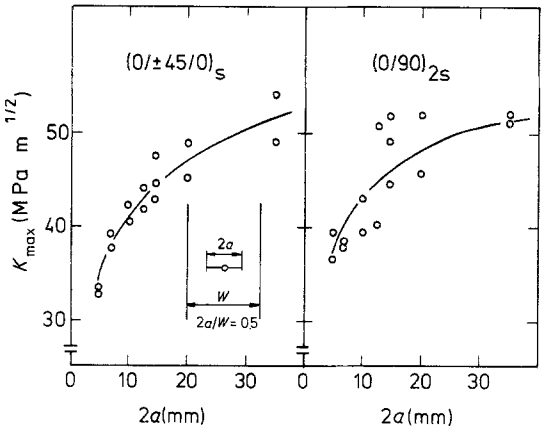

Figure 4 The toughness K_{max} (Equation 2) as a function of the notch length $2a$ of centre-notched $(0/\pm 45/0)_s$ and $(0/90)_{2s}$ specimens.

notch lengths is probably due partly to specimen size effects. The ligament of the smallest specimen is too small for the stress increase at the notch tips to be able to damp up to the specimen edges. Nevertheless it must be concluded that d_0 and a_0 are not material constants but depend upon the notch length. A similar result has been reported by Prabhakaran [10] who found that, for bidirectional glass–epoxy, d_0 and a^*, the inherent flaw size in the WEK model, also depend upon the hole size.

From strain measurements on double-edge-notched, unidirectional boron–Aluminium composite, it was concluded [18] that with increasing notch length the stress very close to the notch tip lags behind the theoretical stress distribution. This causes increasing characteristic lengths at larger notch lengths. It is to be expected that in graphite–epoxy laminates, the stress distribution at the notch tip flattens due to the extending damage at the notch tip at increasing notch length, resulting in the larger characteristic lengths.

As the inherent flaw size a^* is related to the characteristic length a_0 by $a^* = a_0/2$ [9], it is clear from Fig. 5 that a^* increases with increasing notch length. The dependency of the characteristic lengths on notch length in the point and average stress criteria and the WEK model make these fracture-mechanic approaches for the materials investigated questionable.

3.3. K_R curves

The load–COD records were initially linear but deviated from linearity as the damage zone grew ahead of the crack tip, as shown in Fig. 1. Initial straight-line portions at various initial crack lengths were used to calculate the compliance. The compliance as a function of $2a/W$ was fitted to a polynomial by a least-squares estimate, with the best-fit third degree polynomial. The effective crack length, using this compliance calibration curve, was obtained for calculation of K_R at various load levels. Crack growth resistance is calculated from

$$K_R = \sigma Y(\pi a)^{1/2} \qquad (7)$$

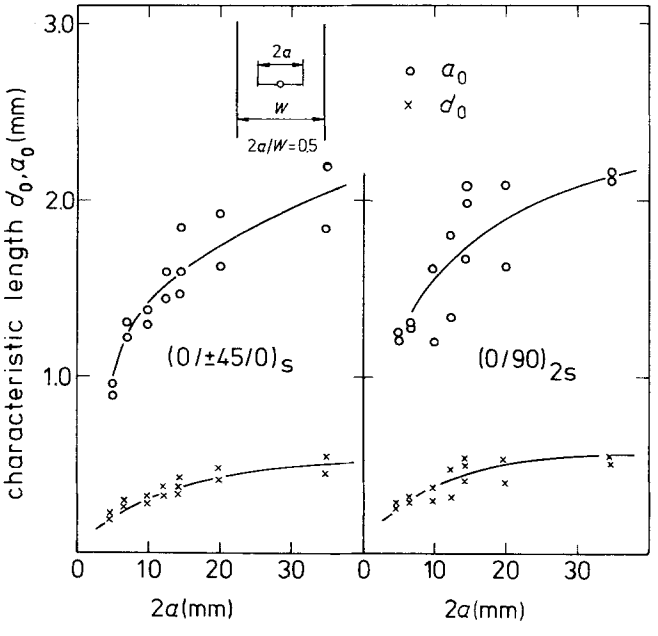

Figure 5 The characteristic lengths a_0 and d_0 as the function of the notch length $2a$ of the centre-notched $(0/\pm 45/0)_s$ and $(0/90)_{2s}$ specimens.

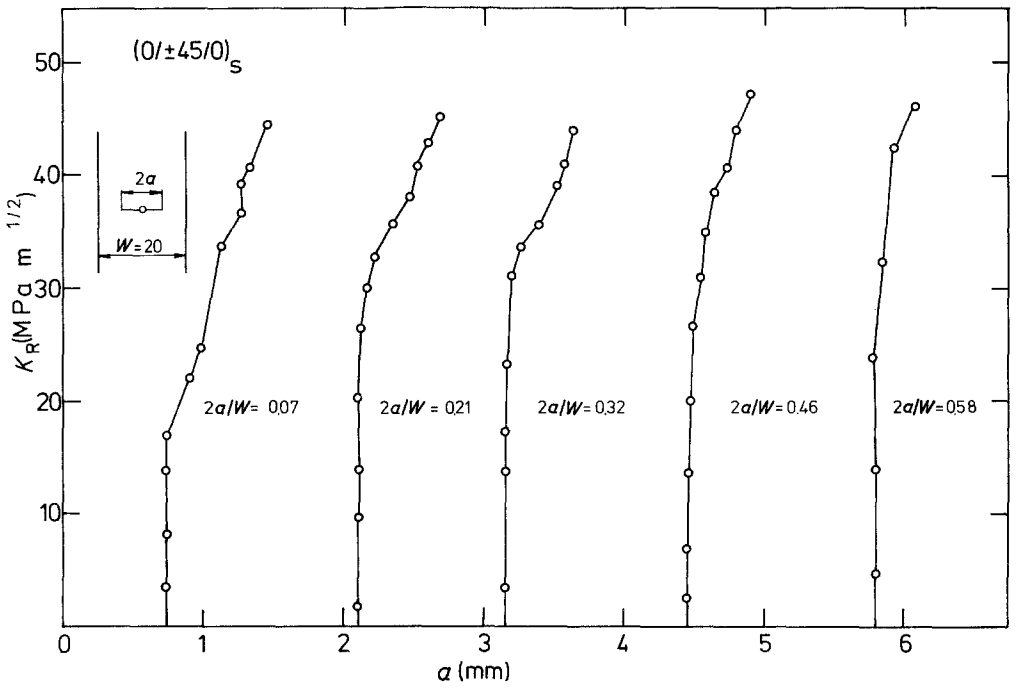

Figure 6 K_R curves of centre-notched $(0/\pm 45/0)_s$ specimens ($W = 20$ mm) with different half-notch length a ($0.7 \leqslant a \leqslant 5.8$ mm).

where σ and a are nominal stress and effective half-crack length and Y is a finite-width correction factor based on effective crack length. Figs 6 and 7 depict the relationship between crack-growth resistance and effective crack length for the $(0/\pm 45/0)_s$ and $(0/90)_{2s}$ laminates with changing relative notch length $2a/W$ at a constant width, $W = 20$ mm. In the $(0/\pm 45/0)_s$ laminate the

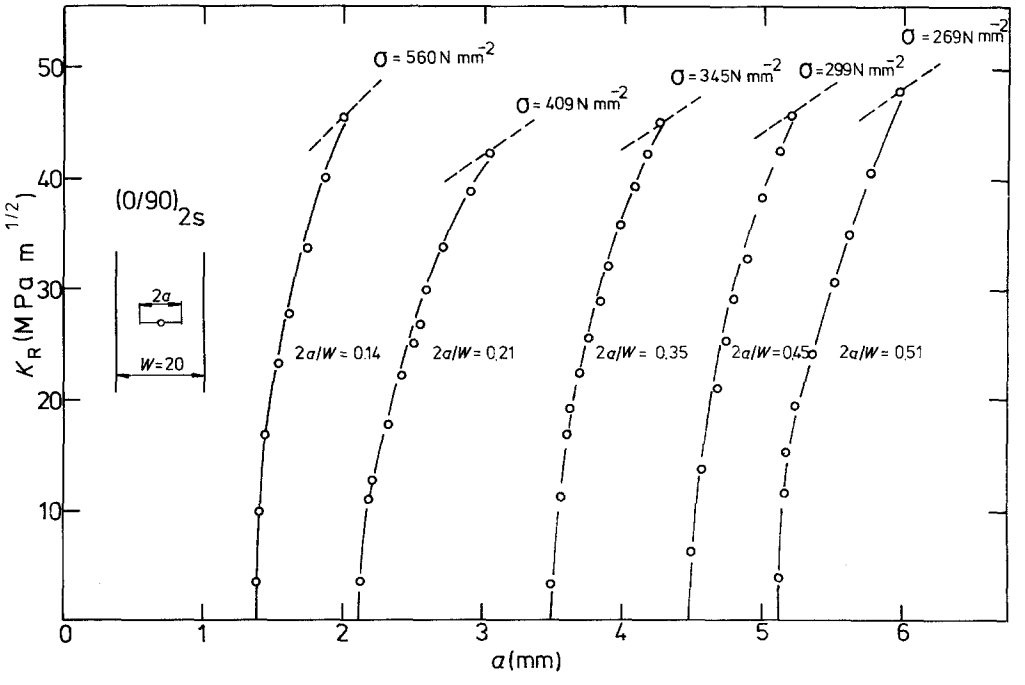

Figure 7 K_R and K curves of centre-notched $(0/90)_{2s}$ specimens ($W = 20$ mm) with different half-notch length a ($1.4 \leqslant a \leqslant 5.1$ mm).

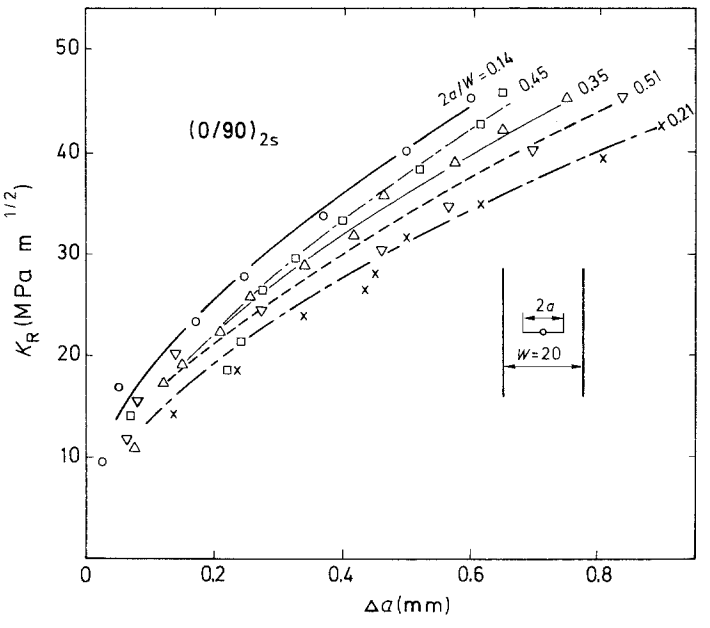

Figure 8 $K_R-\Delta a$ curves of centre-notched $(0/90)_{2s}$ specimens ($W = 20$ mm) with different relative notch length $2a/W$.

damage zone developed suddenly causing steps in the K_R curve, whereas in the $(0/90)_{2s}$ laminate, the damage zone grew continuously resulting in smooth K_R curves.

If the crack-growth resistance curve is a material property, the shape and nature of the curve should be unaltered at various crack lengths. Because of the irregular shape of the K_R curves of the $(0/\pm 45/0)_s$ laminate (Fig. 6), further effort was only expended on the $(0/90)_{2s}$ laminate. The K_R curves of the $(0/90)_{2s}$ laminate seem to be independent of the initial crack length. This is shown in Fig. 8, which presents the $K_R-\Delta a$ curves at different relative crack length, where Δa refers to an extension of the crack. The curves, however, are subject to large scatter.

According to the K_R curve concept, the ultimate failure stress can be determined by the point of tangency between K_R in Equation 7 and the K curve defined by $K = \sigma Y(\pi a)^{1/2}$ with σ as a parameter. Fig. 7 shows that a tangent point between the K_R curve and K curve at the ultimate stress does not exist. Morris and Hahn [7] came to the same result investigating $(0/\pm 45)_s$ and $(0/90/\pm 45)_s$ graphite–epoxy composites.

Because of the lack of a tangent point, the K_R curve seems to be of no use for the prediction of a critical stress of notched laminates. Fig. 9, however, indicates that the maximum fracture resistance $K_{R_{max}}$ is independent of the notch length. This could be a simpler fracture criterion than the one based on a tangent point between K_R and K curves. The K_R curves of the $(0/\pm 45/0)_s$ laminate show the same tendency. When all test results are considered, as presented in Fig. 9, a tendency to a small increase in $K_{R_{max}}$ with rising notch length can be found for both $(0/\pm 45/0)_s$ and $(0/90)_{2s}$ laminates.

Investigations on $(0/90)_{2s}$ specimens with various notch lengths ($5 \leqslant 2a \leqslant 35$ mm at $2a/W = 0.5$) again indicate that the K_R curve is a material property. This is shown in Fig. 10, which presents $K_R-\Delta a$ curves for different notch lengths. With these specimens again no tangent point between

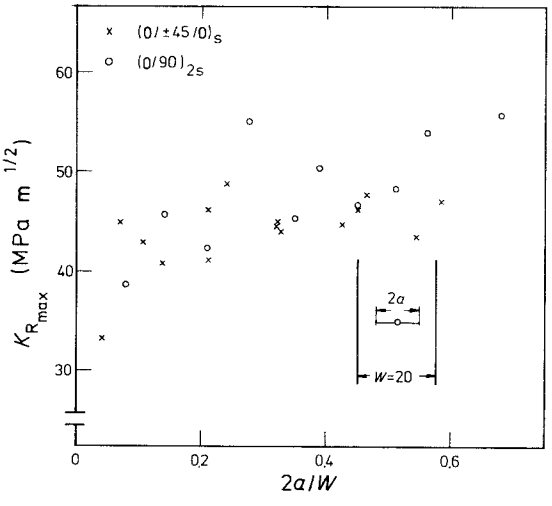

Figure 9 The maximum fracture resistance $K_{R_{max}}$ as a function of the relative crack length $2a/W$ ($W = 20$ mm) for the $(0/\pm 45/0)_s$ and $(0/90)_{2s}$ laminates.

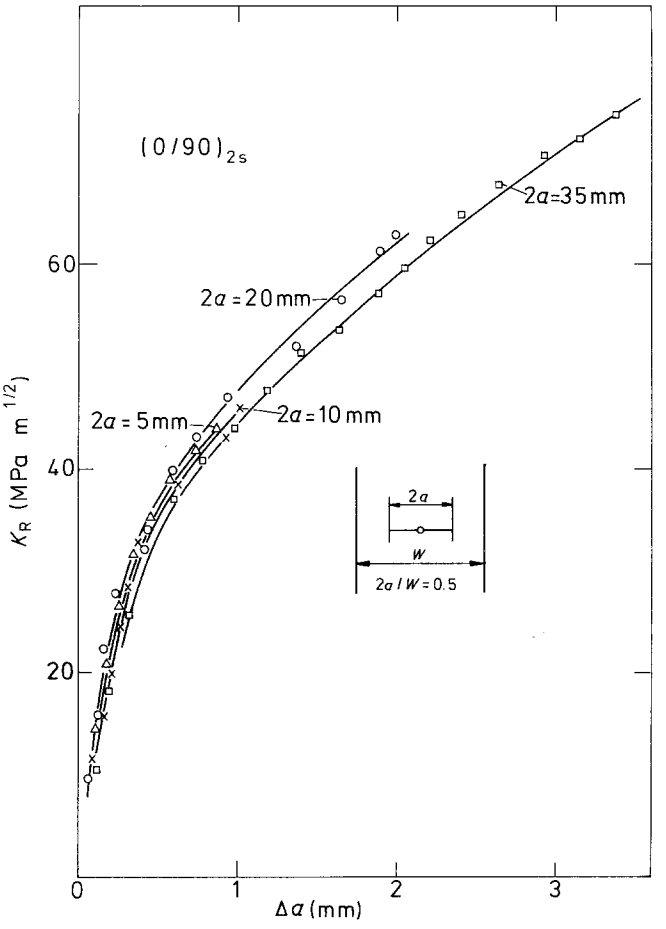

Figure 10 K_R Δa curves of centre-notched $(0/90)_{2s}$ specimens $(2a/W = 0.5)$ with different notch length $2a$.

the K_R and K curves at the critical stress (Fig. 11) could be found. This supports the suggestion made before that the K_R curve cannot be used to predict the critical stress by the aid of a tangent point between K_R and K curves. Besides, $K_{R_{max}}$ is clearly dependent on the notch length. Thus, $K_{R_{max}}$ is of no use in predicting the fracture stress of these notched laminates.

Morris and Hahn [7] and Kim[11] found that the characteristic length d_0 is comparable to the quasi-crack extension at fracture Δa_f. The experiments on notched, 20 mm wide specimens show

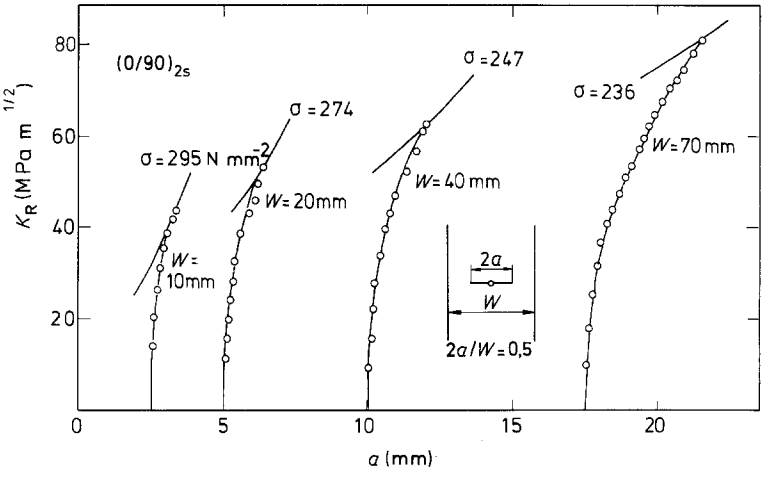

Figure 11 K_R and K curves of centre-notched $(0/90)_{2s}$ specimens $(2a/W = 0.5)$ with different half-notch length a $(2.5 \leqslant a \leqslant 17.5$ mm).

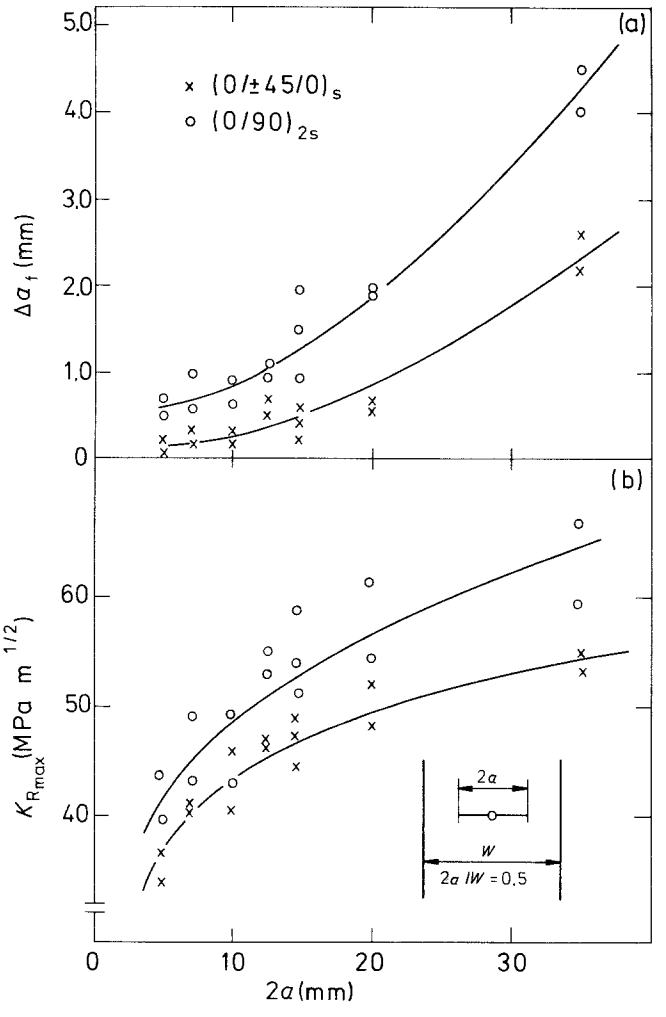

Figure 12 The maximum fracture resistance $K_{R_{max}}$ and the (quasi) crack extension at fracture Δa_f of centre-notched $(0/\pm45/0)_s$ and $(0/90)_{2s}$ specimens ($2a/W = 0.5$).

that in the case of the $(0/\pm 45/0)_s$ laminate the quasi-crack extension at fracture Δa_f is larger or equal to the characteristic length d_0 (Fig. 3). The values of Δa_f of all specimens from laminate $(0/90)_{2s}$, however, are larger than the d_0 values. The experiments at various notch lengths ($5 \leqslant 2a \leqslant 35$ mm at $2a/W = 0.5$) show that the crack extension at fracture Δa_f increases exponentially with rising notch length (Fig. 12). The characteristic length d_0 increases, too, but seems to approach asymptotically a maximum value (Fig. 5). This leads to a growing difference between Δa_f and d_0 at increasing notch length. Therefore Δa_f cannot be directly related to d_0.

One should bear in mind that the crack extension Δa_f is not a real crack extension. The COD increase, which is regarded as the result of the real crack extension in the K_R concept, is, however, mainly the result of the formation of a damage zone (subcracks) at the crack tip. The form of this damage zone are the subject of discussion in the next section.

3.4. Size of the damage zone

The size of the damage zone in specimens with various initial crack lengths at a constant width $W = 20$ mm was observed with X-rays. Typical appearances of the damage zone in both $(0/\pm45/0)_s$ and $(0/90)_{2s}$ laminates are shown in Fig. 13. In the $(0/\pm45/0)_s$ specimens the longitudinal crack in the 0° layer at the notch tip (0° subcrack) was very large, in contrast, the subcrack in the ± 45° layer (45° subcrack) did not extend so far. The specimen from the $(0/90)_{2s}$ laminate also showed subcracks in both fibre directions.

The complex appearances of the damage zone make it difficult to treat them in a quantitative manner. However, we tried to find a parameter which controls the extension of the damage zone. In Figs 14 and 15 the measured sizes of subcracks

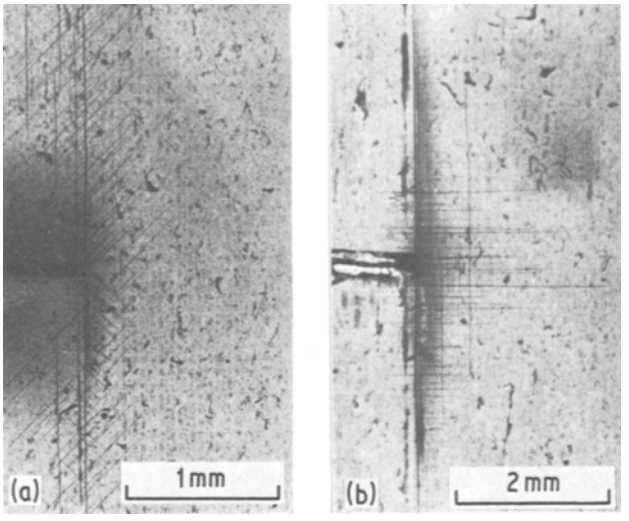

Figure 13 (a) Appearance of the damage zone at 96% failure stress of a notched $(0/\pm45/0)_s$ specimen and (b) at 50% failure stress of a notched $(0/90)_{2s}$ specimen.

are given, where l_0, l_{45} and l_{90} refer to the size of the 0°, ±45° and 90° subcracks, respectively, as shown schematically. As the damage zone could be regarded as the plastic zone in metals, the measured values of l_0, l_{45} and l_{90} were plotted against K^2. It has been reported that the size of each subcrack is proportional to K^2 [17, 19], but in this investigation such a relation was not found.

At a low stress intensity factor ($K^2 < 500$ Mpa^2 m) the $(0/\pm 45/0)_s$ composite deformed elastically with no damage, and no subcrack was observed, as shown in Fig. 14. On the other hand, in the $(0/90)_{2s}$ composite, the subcracks formed at a very low stress intensity factor and they extended more than those in the $(0/\pm 45/0)_s$ composite, as is evident by comparing Fig. 15 with Fig. 14.

The size of the 0° subcrack in $(0/90)_s$ specimens is about two times larger than the 0° subcracks of the $(0/\pm 45/0)_s$ specimens, whereas the 90° subcracks are longer by about a factor of 10 than the ± 45° subcracks. This corresponds to the aforementioned result that the quasi-crack extension at fracture Δa_f of the $(0/\pm 45/0)_s$ composite is smaller than that of the $(0/90)_{2s}$ composite. Due to the large scatter, no conclusive statement on the effect of original crack length on subcrack length could be made.

Fig. 16 gives a direct comparison of l_0 and l_{90} with Δa, which was determined from the compliance matching for the $(0/90)_{2s}$ composite. The subcrack l_0 and l_{90} are much larger than Δa. This figure also shows that a subcrack length increase at a small subcrack length influences the size of Δa more than an increase at higher subcrack length. This indicates that the load transfer

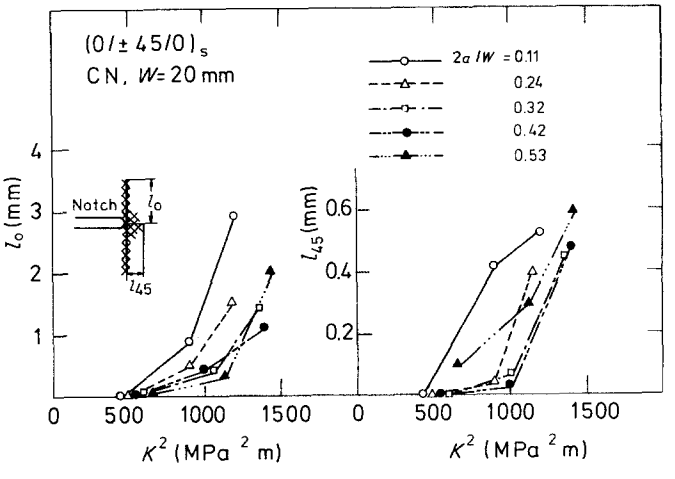

Figure 14 Subcrack length l_0 and l_{45} plotted against K^2 for centre-notched $(0/\pm 45/0)_s$ specimens with different relative notch lengths (W = 20 mm).

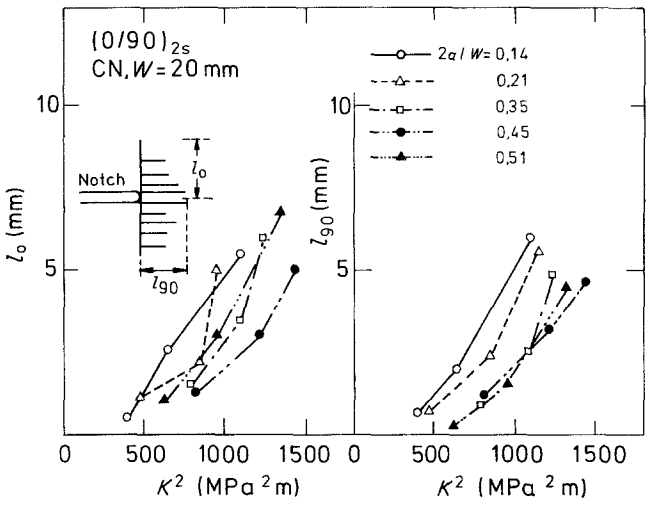

Figure 15 Subcrack length l_0 and l_{90} plotted against K^2 for centre-notched $(0/90)_{2s}$ specimens with different relative notch lengths (W = 20 mm).

at the notch tip with increasing subcrack length more and more takes place through interlaminar stresses.

4. Conclusions

(a) At increasing load, the COD of notched specimens deviates from the original linearity. This is mainly caused by the formation of a damage zone at the crack tips. Subcracks parallel to the fibres of the constituent layers are formed, the size of which were shown not to be proportional to the square of the stress intensity factor K^2. The extension of the damage zone at increasing load in the $(0/90)_{2s}$ laminates is smooth, whereas in the $(0/\pm 45/0)_s$ laminate the damage zone propagates abruptly causing steps in the load–COD curve.

(b) From the load–COD curves, K_R curves were derived by assuming that the deviation from linearity of the load–COD curves is caused by self-similar crack extension (compliance matching). The K_R curves of the $(0/90)_{2s}$ laminate are almost independent of the notch length, which cannot be said for the $(0/\pm 45/0)_s$ laminate. The shape of its K_R curves are irregular as a result of the abrupt extension of the damage zone.

A prediction of the fracture stress of notched $(0/90)_{2s}$ specimens based on the K_R curve proved to be impossible, as a tangent point between K_R and K curves could not be found. In the specimens of both $(0/\pm 45/0)_s$ and $(0/90)_{2s}$ laminates at a constant width, the maximum crack resistance $K_{R\,max}$ seemed to be slightly dependent on notch length. At varying notch length, however, the maximum fracture resistance was clearly dependent on

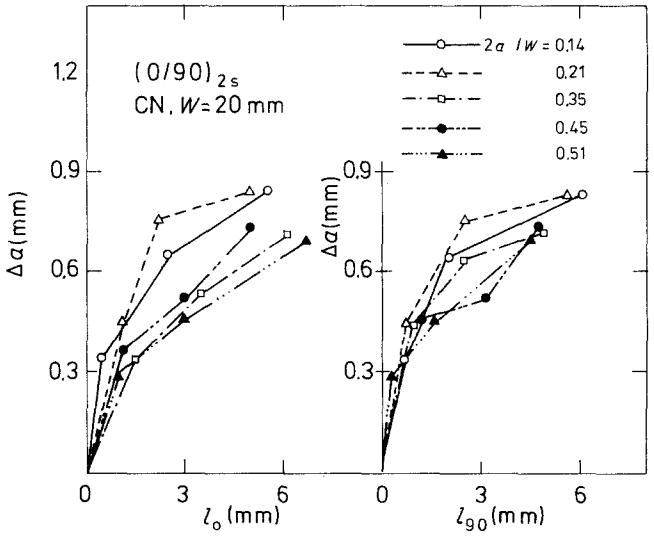

Figure 16 Direct comparison of Δa with l_0 and l_{90} of centre-notched $(0/90)_{2s}$ laminates with different relative notch lengths (W = 20 mm).

the notch length, which shows that $K_{R_{max}}$, too, cannot be used for the prediction of the fracture stress of notched laminates.

(c) The point and average stress criteria were applicable for the notches ($0 < 2a \leqslant 12$ mm) in 20 mm wide specimens of both $(0/\pm 45/0)_s$ and $(0/90)_{2s}$ laminates. The influence of varying notch length ($5 < 2a \leqslant 35$ mm at $2a/W = 0.5$) could, however, not be described with constant characteristic lengths. These lengths clearly rose at increasing notch length. As the Waddoups, Eisenman and Kaminski model is related to the average stress criterion, this model is not able to describe the notch length effect.

Acknowledgement

S. Ochiai wishes to express his gratitude to Professor W. Bunk for his invitation to his Institute and to the Alexander von Humboldt Foundation for financial support for his stay in West Germany.

References

1. M. E. WADDOUPS, J. R. EISENMANN and B. E. KAMINSKI, *J. Comp. Mater.* 5 (1971) 440.
2. J. C. HALPIN, K. L. JERINA and T. A. JOHNSON, "Analysis of the Test Methods for High Modulus Fibres and Composites", ASTM STP 521, (ASTM, Philadelphia, 1973) p. 5.
3. N. R. ADSIT and J. P. WASZACZAK, "Fracture Mechanics of Composites" ASTM STP 593 (ASTM, Philadelphia, 1975) p. 163.
4. J. M. WHITNEY and R. J. NUISMER, *J. Comp. Mater.* 8 (1974) 253.
5. R. J. NUISMER and J. M. WHITNEY, "Fracture Mechanics of Composites", ASTM STP 593 (ASTM, Philadelphia 1975) p. 117.
6. S. GAGGER and L. J. BROUTMAN, *J. Comp. Mater.* 9 (1975) 216.
7. D. H. MORRIS and H. T. HAHN, "Composite Materials", ASTM STP 617 (ASTM, Philadelphia, 1977) p. 5.
8. R. B. PIPES, R. C. WETHERHOLD and J. W. GILLESPIE Jr, *J. Comp. Mater.* **13** (1979) 148.
9. S. W. TASI and H. T. HAHN, "Inelastic Behaviour of Composite Materials", AMD Vol. 13 (ASME, New York, 1975) p. 73.
10. R. PRABHAKARAN, *Mater. Sci. Eng.* **41** (1979) 121.
11. R. Y. KIM, *Exp. Mech.* (1979) 50.
12. J. F. MANDELL, S. S. WANG and M. J. McGARRY, Air Force Materials Laboratory Technical Report AFML-TR-73-142 (1973).
13. F. H. CHANG, J. C. COUCHMAN, J. R. EISENMANN and B. G. W. YEE, "Composite Reliability", ASTM STP 580 (ASTM, Philadelphia, 1975) p. 176.
14. M. D. SNYDER and T. A. CRUSE, Air Force Materials Laboratory Technical Report AFML-TR-73-209 (1973).
15. T. A. CRUSE and J. R. OSIAS, Air Force Laboratory Technical Report AFML-TR-74-111 (1974).
16. C. E. FEDDERSON, "Discussion", ASTM STP 410 (ASTM, Philadelphia, 1967) pp. 77–79.
17. J. F. MANDELL, S. S. WANG and F. J. MCGARRY, Air Force Materials Laboratory Technical Report, AMFL-TR-74-167, (1974).
18. P. W. M. PETERS, in "Advances in Composite Materials" Proceedings of the Third International Conference on Composite Materials, Paris, August 1980, edited by A. R. Bunsell *et al.* (Pergamon Press, Oxford and New York, 1980) p. 1153.
19. J. F. MANDELL, S. S. WANG and F. J. MCGARRY, *J. Comp. Mater.* 9 (1975) 266.

Received 12 May
and accepted 3 July 1981